# Spatial and Temporal Visualization of Two Aqueous Iron Oxidation–Reduction Reactions by Nuclear Magnetic Resonance Imaging

**Bruce J. Balcom,* T. Adrian Carpenter and Laurance D. Hall**

*Herchel Smith Laboratory for Medicinal Chemistry, School of Clinical Medicine, University of Cambridge, Robinson Way, Cambridge CB2 1PZ, UK*

$^1$H Nuclear magnetic resonance imaging is used to follow the progress of two dispersion-limited chemical reactions, oxidation and reduction of iron, in a simple polyacrylamide gel system.

Although it is general practice in chemical kinetics to stir reagents to ensure that a reaction is homogeneous, for many physical processes, particularly in viscous media, such mixing is either inefficient or not feasible. The purpose of this communication is to examine, by nuclear magnetic resonance imaging (NMRI),[1–3] two systems, an oxidation and a reduction, for which the overall reaction kinetics are limited by the dispersion of one of the reagents. These systems are particular examples of a larger class of problems the behaviour of which is controlled by the reaction–diffusion equation.[4]

The problem of producing a well-defined concentration front between two reagents is well known from studies of free diffusion in aqueous media.[5] In this study we have exploited polyacrylamide gels to limit adventitious mixing of the reagents by long range convection.[6,7] The gels† (90% water) were cast as right cylinders of polyacrylamide with a 5 mm diameter void, concentric with the cylinder axis, from which dispersion of reagent is controlled by diffusion. The irreversible chemical reactions are mapped in space and time by NMRI of the water protons, utilizing aqueous iron species as an indicator. The migration of reactant from the axial void is indirectly observed by its alteration of the $Fe^{2+}/Fe^{3+}$ redox couple. The sodium bromate oxidation‡ and the ascorbic acid reduction of aqueous iron[8] both proceed rapidly at pH 1. The reaction fronts observed in Figs. 1 and 2 are thus predominantly controlled by dispersion of the reagent, not the thermodynamics of their reaction.

A $T_1$-weighted§ spin warp NMR imaging sequence[9] (fast repetition rate, short $T_E$) maps the distribution of $Fe^{2+}$ and $Fe^{3+}$ species as a function of space and time due to their differential effects on the relaxation times of water protons in the gel. The analytical expression for the signal intensity at any point in the image is given by eqn. (1). $T_E$ is the time until the spin echo is detected, $T_R$ is the repetition time, and $\rho$ is proton density. $T_1$ and $T_2$ are, respectively, the longitudinal and spin–spin nuclear relaxation times of the water protons in the gel.

$$S = \rho e^{(-T_E/T_2)} (1 - e^{(-T_R/T_1)}) \quad (1)$$

Bulk sample inversion recovery measurements of water in the gel gave a $T_1$ value of 1.1 s in the presence of $Fe^{2+}$ (1 mmol $dm^{-3}$; pH 1), and 0.075 s in the presence of $Fe^{3+}$ under the same conditions, reflecting their different electron spin relaxation times.[10] Contrast in these experiments originates primarily from the second exponential of eqn. (1) due to a spatial variation of $T_1$. While the $T_2$ of the water protons is somewhat attenuated by the paramagnetic iron, a short $T_E$ means the spatial variation in signal due to the first exponential in eqn. (1) is minimized. Under these conditions a $T_R$ chosen between the two extremes of $T_1$ will give image contrast. A small difference in $T_1$, however, will yield a difference in signal intensity, which may be difficult to discern in a low signal to noise image. In these systems the signal to noise is very good and the variation in $T_1$ is large so contrast is easily discerned.

Reactions were commenced by adding a pH 1 aqueous solution of the appropriate oxidant–reductant to the void in the presence of a pH 1 aqueous solution of $Fe^{2+}$ or $Fe^{3+}$ in the gel. Fig. 1 shows two transverse slice images from the middle of the cylinder acquired 15 and 45 min after initiation of the

† Polyacrylamide gels were formed, over 24 h, from a 90:9.5:0.5 mixture of water, acrylamide and bis(acrylamide), using ammonium persulfate as initiator and *N,N,N′,N′*-tetramethylenediamine as accelerator.[6] Gels were cast as right cylinders of diameter 26 mm in a perspex cylinder 40 mm in height sealed at the bottom, with a 5 mm NMR tube placed concentric with the cylinder axis. Cylindrical symmetry of the sample permits a large slice thickness in the imaging experiment and an attendant increase in the signal to noise ratio. Water-soluble byproducts of the reaction were removed by equilibration in a large reservoir of distilled, deionized water. Gels were doped, by pre-equilibration, with 1 mmol $dm^{-3}$ sulfate salts of $Fe^{2+}$ and $Fe^{2+}$ at pH 1.

‡ Homogeneous test reaction at concentrations representative of this work. Phenanthroline indicator.

§ Samples for study were inserted into a 26 mm internal diameter perspex cylinder sealed at the bottom, located inside a modified split ring resonator[14] NMR probe of 5 cm diameter. Reaction was commenced by addition of 100 mmol $dm^{-3}$ sodium bromate, or ascorbic acid, at pH 1, to the axial void. The imaging experiment was performed using an Oxford Research Systems Biospec 1 (84.7 MHz) instrument with an Oxford Instruments horizontal bore (31 cm) magnet, and 20 cm home built gradient set. The spin-warp sequence,[9] with a hard 90° pulse and slice selective 180° pulse, had a repetition time of 0.5 s and an echo time of 13 ms. Slice thickness was 1 cm and two signal averages were collected for each 256 × 256 image. Acquisition time for each image was five min. Pixel resolution was 0.2 mm with a field of view of 5 cm. Resolution in the region of transition between $Fe^{2+}$ and $Fe^{3+}$ is substantially less than this owing to movement of the reaction front during image acquisition. Assuming a sharp reaction front with a linear velocity between the timed images in Figs. 1 and 2, there will be a blurring of the image in this region by approximately 10 pixels in Fig. 1 and 2 pixels in Fig. 2. This estimate is conservative at short reaction times when the front moves quickly.

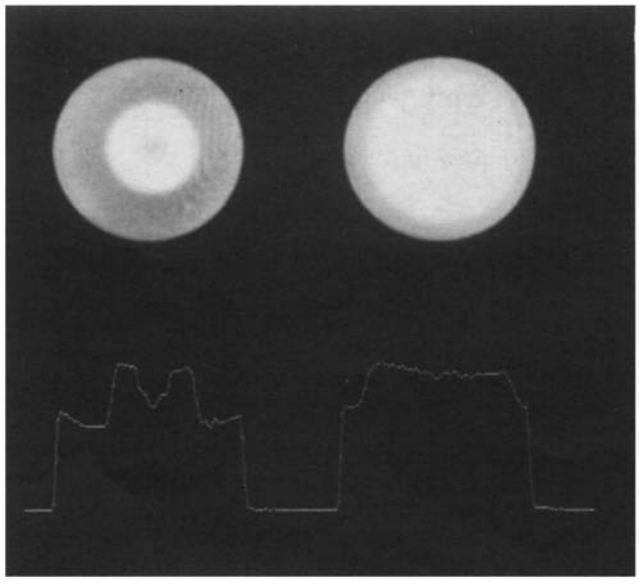

Fig. 1

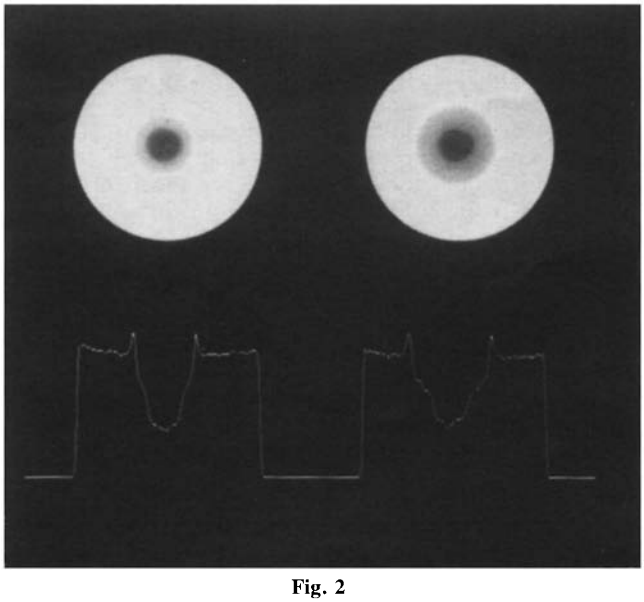

Fig. 2

oxidation reaction. Regions of the sample where $Fe^{2+}$ has been converted to $Fe^{3+}$ give the most intense signal. Those regions without significant concentrations of $Fe^{3+}$ give a less intense signal because the long relaxation times of water in this environment, under the influence of a relatively rapid, repetitive radio frequency pulse, yields a steady-state longitudinal magnetization, which is restricted in magnitude. A short time after initiation of the reaction, areas of low intensity include the axial void itself and regions of the gel a moderate distance from the void. As time progresses, diffusion of $Fe^{3+}$ into the central void decreases the $T_1$ of water in this region and the image intensity increases. The spatial variation of intensity in this void (left image, Fig. 1) shows a concentration gradient of $Fe^{3+}$ has been established in free solution.

The reduction reaction is visualized in Fig. 2 which shows two transverse slice images from the middle of a different cylinder, 15 and 50 min after initiation of the reaction. Again, regions of the sample with large signal intensities correspond to significant $Fe^{3+}$ concentrations, while those without have a lower image intensity. The gross structural features of this sample are similar to those of Fig. 1 (with inverted relative intensities) except for the sharp spike of high intensity which precedes the reduction wave. This spike may result from phenomena occurring at the reaction front, for example an attendant change in temperature or it may be an imaging artifact. Initial studies with a fast imaging protocol employing gradient recalled echoes, rather than spin echoes, do not show this spike.

The reaction kinetics of systems such as these may fall into three regimes. (*i*) Slow reaction. If the reagents mix before they react we have a simple homogeneous system with no spatial discrimination. (*ii*) Intermediate reaction rate. Both diffusion and reaction kinetics determine the position and shape of the reaction front with time.[11] (*iii*) Fast reaction. If the rate of reaction is very fast, then the reaction is entirely limited by diffusion and the reaction front will move (in one dimension) proportional to the square root of time. Roughton[11] has estimated that if the half time of the pure reaction is at least 100 times less than the half time of the observed process, then the spread of the reaction will be diffusion controlled. For these systems (half time approximately 30 min) we may estimate that pseudo-first-order rate constants of less than 0.04 $s^{-1}$ will be required before the kinetics of the reaction influence the observed reaction front. This limit is dependent on the sample size.[11]

Static systems similar to those illustrated by Figs. 1 and 2 are amenable to quantification by NMRI in terms of proton density and $T_1$, $T_2$ relaxation times.[1,12,13] A more complete consideration of dynamic systems such as those examined here in terms of rate constants and/or mass transport coefficients, however, requires a much shorter imaging time to 'freeze' the movement of the reaction zone and permit examination of the concentration gradient (*via* $T_1$ variation) as a function of time. Further work in these areas using one-dimensional samples will be forthcoming. Nevertheless, the key general feature of this work is that it demonstrates one means by which the spatial and temporal variations of the reaction of a species present in a concentration below the normal level of NMR detectability can be visualized by NMRI. Similar studies can be made of the creation, destruction or alteration of paramagnetic species such as free radicals, providing that these are present in sufficiently high concentration to yield a differential in nuclear relaxation times of the solvent.

We thank Dr Herchel Smith for a generous endowment (T. A. C., L. D. H.) and NSERC of Canada for a postdoctoral fellowship (B. J. B.).

*Received, 11th September 1991; Com. 1/04727B*

## References

1 J. Attard, L. Hall, N. Herrod and S. Duce, *Physics World*, 1991, **4**, 41.
2 A. J. S. de Crespigny, T. A. Carpenter, L. D. Hall and A. G. Webb, *Polym. Commun.*, 1990, **32**, 36.
3 A. Tzalmona, R. L. Armstrong, M. Menzinger, A. Cross and C. Lemaine, *Chem. Phys. Lett.*, 1990, **174**, 199.
4 J. Crank, *The Mathematics of Diffusion*, OUP, Oxford, 1989, ch. 14.
5 O. Bryngdahl, *Acta Chem. Scand.*, 1958, **12**, 684.
6 A. T. Andrews, *Electrophoresis: Theory, Technique, and Biochemical and Clinical Applications*, Oxford Science, Oxford, 1986, ch. 2.
7 T. Yamaguchi, L. Kuhnert, Zs. Nagy-Ungvarai, S. C. Muller and B. Hess, *J. Phys. Chem.*, 1991, **95**, 5831.
8 R. D. Perry and C. L. San Clemente, *Analyst*, 1977, **102**, 114.
9 W. A. Edelstein, J. M. Hutchinson, G. Johnson and T. Redpath, *Phys. Med. Biol.*, 1980, **25**, 751.
10 J. C. Gore, Y. S. Kang and R. J. Schuly, *Phys. Med. Biol.*, 1984, **29**, 1189.
11 F. J. W. Roughton, *Prog. Biophys. and Biochem.*, 1959, **9**, 55.
12 P. A. Osment, K. J. Packer, M. J. Taylor, J. J. Attard, T. A. Carpenter, L. D. Hall, N. J. Herrod and S. J. Doran, *Phil. Trans. R. Soc. Lond. A*, 1990, **333**, 441.
13 C. F. Jenner, Y. Xia, C. D. Eccles and P. T. Callaghan, *Nature*, 1988, **336**, 399.
14 L. D. Hall, T. Marcus, C. Neale, B. Powell, J. Sallos and S. L. Talagala, *J. Magn. Reson.*, 1985, **62**, 525.